

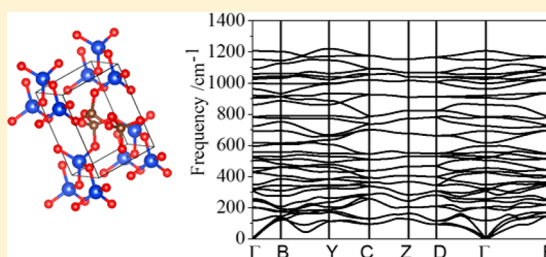
# Mechanism of Chemical Reactions between SiO<sub>2</sub> and CO<sub>2</sub> under Mantle Conditions

Xue Yong,<sup>†</sup> John S. Tse,<sup>\*,†,‡,§</sup> and Jiu-hua Chen<sup>§,||</sup>HPSTAR  
589-2018<sup>†</sup>Department of Physics and Engineering Physics, University of Saskatchewan, Saskatoon, Saskatchewan, Canada S7N 5E2<sup>‡</sup>State Key Laboratory for Superhard Materials, Jilin University, Changchun, China 130012<sup>§</sup>Center for High Pressure Science and Technology Advanced Research, Changchun, China 130015<sup>||</sup>Center for the Study of Matter at Extreme Conditions, Florida International University, Miami, Florida 33199, United States

## Supporting Information

**ABSTRACT:** Silica (SiO<sub>2</sub>) is a major component of many minerals on the Earth. Under ambient conditions, silica does not react with carbon dioxide (CO<sub>2</sub>). However, at high pressure and temperature, the stability of silica may be affected by CO<sub>2</sub>, which becomes supercritical fluid CO<sub>2</sub> under extreme conditions and can percolate into the Earth's mantle to react with silica. Here, we investigated the chemical reactions between zeolite SSZ-56 as a model silicate and CO<sub>2</sub> under temperature and pressure conditions close to those of the mantle transition zone using density functional theory and molecular dynamics calculations. The reactions occurred on the SiO<sub>2</sub> surface forming the zeolite's cavities. In the melt, CO<sub>2</sub> and SiO<sub>2</sub> mixed closely and, upon cooling, formed a solid with disordered Si and C sites similar to a cristobalite SiO<sub>2</sub>-CO<sub>2</sub> solid-solution structure. This structure was thermodynamically stable with respect to  $\alpha$ -cristobalite and solid CO<sub>2</sub> above 9 GPa.

**KEYWORDS:** silica, DFT, chemical reaction, high pressure, Earth's mantle, mineral



## 1. INTRODUCTION

Carbon dioxide and silica are two fundamental components of the Universe. Both are group IV oxides. Molecular CO<sub>2</sub> is the main greenhouse gas, and the current amount in the Earth's atmosphere has become a severe challenge to human life. The presence of CO<sub>2</sub> in the Earth's mantle also plays an important role in volcanic and seismic activities. The CO<sub>2</sub> molecule has strong C=O bonds, so it is chemically inert under ambient conditions. However, the  $\pi$  bond and the properties of CO<sub>2</sub> can be significantly affected by pressure.<sup>1</sup> At low pressures, CO<sub>2</sub> crystallizes into several van der Waals molecular solids. At high pressures and high temperatures (>41 GPa and >1800 K), the CO<sub>2</sub> molecules rehybridize and transform into an extended solid with single (sp<sup>3</sup>) bonded C-O<sup>1</sup> sharing a similar structure with the  $\beta$ -cristobalite polymorph of SiO<sub>2</sub>. In addition, CO<sub>2</sub> fluid becomes supercritical, when it is held above its critical temperature and critical pressure, and can percolate into most materials. Under ambient conditions, CO<sub>2</sub> and SiO<sub>2</sub> do not react with each other, but reactivity is expected to be promoted by high pressures and high temperatures. The similarity between CO<sub>2</sub> and SiO<sub>2</sub> at high pressures has stimulated several recent studies to investigate the possible reactions between them.<sup>2,3</sup> Such chemical reactions, on one hand, are of fundamental importance for understanding the deep carbon cycle; on the other hand, such reactions may have important practical applications. For example, injecting CO<sub>2</sub> underground has been proposed as a new and efficient way of removing extra

CO<sub>2</sub> from the atmosphere.<sup>4–6</sup> The possibility of forming three-dimensional extended covalent solids may help stabilize the reaction products that, in themselves, may even be potential candidates as high-energy content materials. In fact, silicon-oxygen polyhedra bonded to carbonates have been found in carbon bearing silicate melt.<sup>7</sup> The exploration of the chemical reaction between CO<sub>2</sub> and SiO<sub>2</sub> at high pressures will help the development of new chemistry between these two chemical species. However, experimental and theoretical studies on this subject are limited.<sup>2,3,8–10</sup>

Santoro et al.<sup>2</sup> reported the first observation of a disordered silicon carbonate formation by compressing a sample of microporous silica (zeolite) with CO<sub>2</sub>-filled voids at pressures of 18–26 GPa and temperatures between 600 and 980 K. No detailed information about the structure or the reaction mechanism was presented. Later, the same group<sup>3</sup> reported the observation of a SiO<sub>2</sub>-CO<sub>2</sub> solid solution from the reaction of CO<sub>2</sub> and a silica melt at pressures around 16–22 GPa and temperatures of >4000 K. The report was challenged.<sup>3,11,12</sup> Here, we propose a novel mechanism on the formation of a SiO<sub>2</sub>-CO<sub>2</sub> solid solution. We have undertaken a theoretical investigation of the reactions between CO<sub>2</sub> and porous zeolite

Received: December 12, 2017

Revised: March 5, 2018

Accepted: March 19, 2018

Published: March 19, 2018

SSZ-56  $\text{SiO}_2$  under mantle transition zone conditions using density functional (DFT)-based *ab initio* molecular dynamics (AIMD) simulations and total energy calculations. The theoretical results helped to identify the reaction products and provide an atomistic description of the reaction mechanisms. We also performed a detailed investigation of the structure and energy of the reaction product obtained from quenching the silica melt and  $\text{CO}_2$  and the potential cristobalite  $\text{SiO}_2\text{-CO}_2$  solid solution at high pressures.

## 2. COMPUTATIONAL METHODOLOGY

We investigated the chemical reaction of  $\text{CO}_2$  in SSZ-56 with AIMD calculations. The computational model was constructed from a unit cell of the zeolite SSZ-56,<sup>2,13</sup> a member of the SFS zeolite family with a crystal structure consisting of 56  $\text{SiO}_2$  molecules that is structurally similar to the zeolite used in the experiment. The empty zeolite structure was optimized at 0 GPa, and afterward, 40  $\text{CO}_2$  molecules were inserted into the channels (Figure 1) to create the same chemical composition as

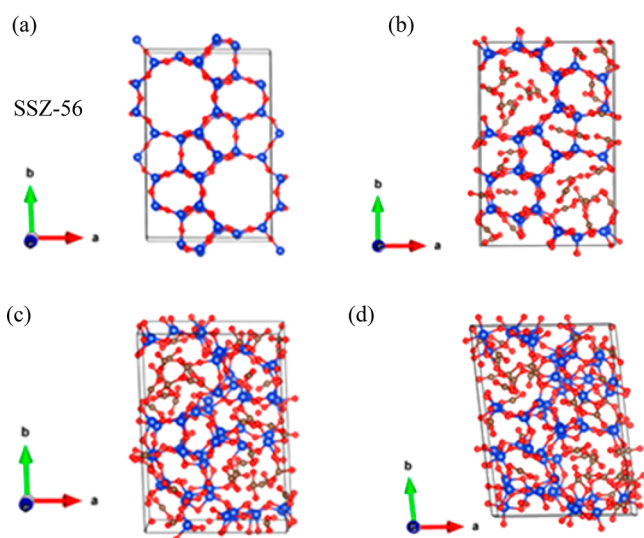


**Figure 1.** (a) Structure of empty SSZ-56. (b) Final snapshot of SSZ  $\text{SiO}_2\text{-CO}_2$  after *NVT* MD simulation at 0 GPa and 100 K and *NPT* MD simulation at (c) 26 GPa and 1000 K and (d) 30 GPa and 500 K (Si, blue; C, gray; O, red).

that of the system studied in the experiment. Therefore, the model consisted of 56  $\text{SiO}_2$  and 40  $\text{CO}_2$  molecules and 288 atoms in total. Following the experimental conditions,<sup>2</sup> the zeolite  $\text{SiO}_2\text{-CO}_2$  model system was equilibrated for 3 ps at 500 K and then to 1000 K at 0 GPa with microcanonical ensemble constant-volume constant-temperature (*NVT*) MD simulations using a Nosé–Hoover thermostat to control the temperature. After equilibration, an isobaric–isothermal canonical ensemble (*NPT*) MD calculation was performed under the experimental condition<sup>2</sup> of 26 GPa and 1000 K. In the *NPT* simulation, the Parrinello–Rahman barostat and Langevin thermostat are employed to control the pressure and temperature, respectively. A fictitious mass of 10 is employed for lattice degrees of freedom. To assess the effects of pressure and temperature, an additional calculation was performed at 30 GPa and 500 K. In each case, the MD simulation lasted for at least 13 ps. To ensure that the reaction was complete, a total 25 ps *NPT* simulation was performed for the system at 26 GPa and 1000 K. Notably, the pressure and temperature considered here

are far below those of the molecular to nonmolecular transformation of  $\text{CO}_2$  (41 GPa and 1800 K, respectively).

To test the hypothesis of  $\text{SiO}_2\text{-CO}_2$  solid-solution formation under high pressures,<sup>3</sup> we examined the structure of the quenched melt of the SSZ-56  $\text{SiO}_2\text{-CO}_2$  model by melting the structure at 25 GPa and 4000 K and then quenching it to 500 K. In addition, the stability of a potential  $\text{SiO}_2\text{-CO}_2$  solid solution structure was constructed from crystalline  $\alpha$ -cristobalite  $\text{SiO}_2$  by randomly replacing half of the Si atoms with C atoms. Static geometry optimization at different pressures was performed. The infrared and Raman spectra, electronic band structure, optical spectrum, elastic modulus, and hardness of this  $\alpha$ -cristobalite  $\text{SiO}_2\text{-CO}_2$  solid solution were calculated. The optical spectrum was computed by solving the Bethe–Salpeter equation (BSE) using *GW*-corrected eigenvalues. The elastic constants were computed by the strain–stress method, and the bulk modulus and shear modulus were derived from the Voigt–Reuss–Hill averaging scheme.<sup>14,15</sup>

All calculations were performed with the Vienna *ab initio* simulation package, VASP,<sup>16–19</sup> which is a plane wave basis electronic structure code using projected augmented (PAW) wave potentials for the atoms. An energy cutoff at 400 eV is used for the plane wave basis set expansion. The PAW<sup>20</sup> treats 3s and 3p orbitals of Si, 2s and 2p orbitals of O, and C atoms as valence electrons. The Perdew–Burke–Ernzerhof (PBE) exchange–correlation functional<sup>21</sup> was employed. An  $8 \times 8 \times 8$  Monkhorst–Pack *k*-point mesh was used to sample the Brillouin zone for geometry optimization, and energy calculations on the  $\text{SiO}_2\text{-CO}_2$  solid solution with the total energy converged to better than 1 meV/atom. A single  $\Gamma$  point was used for Brillouin zone sampling for MD calculation. A time step of 1.0 fs was used to integrate the equations of motion in MD calculations. The MD trajectories were examined to identify the reaction mechanisms and products.

## 3. RESULTS AND DISCUSSION

**3.1. Reaction of  $\text{CO}_2$  Trapped in the Zeolite SSZ-56 Cavities.** Silicalite zeolites are microporous and can be synthesized with pores of different sizes formed from linking of four-, five-, six-, and ten-membered channels formed by  $\text{SiO}_4$  tetrahedra. The porous framework structures can be filled with small molecules through physical absorption.<sup>22</sup> This unique property has been exploited industrially for gas separation and storage.<sup>23</sup> As reported elsewhere,<sup>24</sup> the chemical reaction between  $\text{CO}_2$  and mineral quartz and stishovite proceeds only at the interface. Compared to these minerals, microporous  $\text{SiO}_2$  has a much larger surface and channel to accommodate the  $\text{CO}_2$  molecules. The large surface area of the cavities exposed to the encaged  $\text{CO}_2$  molecules may facilitate reactions at lower pressures and temperatures. Recently, zeolite filled with  $\text{CO}_2$  and compressed under external pressures was studied by infrared spectroscopy, and a disordered silicon carbonate was successfully synthesized at 18–26 GPa and 600–980 K.<sup>2</sup> The objective here is to identify the mechanism and the reaction products with AIMD.

A zeolite (SSZ-56)/ $\text{CO}_2$  model (Figure 1b) with a  $\text{SiO}_2\text{:CO}_2$  ratio close to the experimental stoichiometry was constructed and studied with AIMD. SSZ-56 is made of five-, six-, and ten-membered Si–O channels. During thermal equilibrium, no reaction between the microporous framework and the  $\text{CO}_2$  was uniformly observed (Figure 1b). Upon compression to 26 and 30 GPa using *NPT* MD simulation, the lattice constants

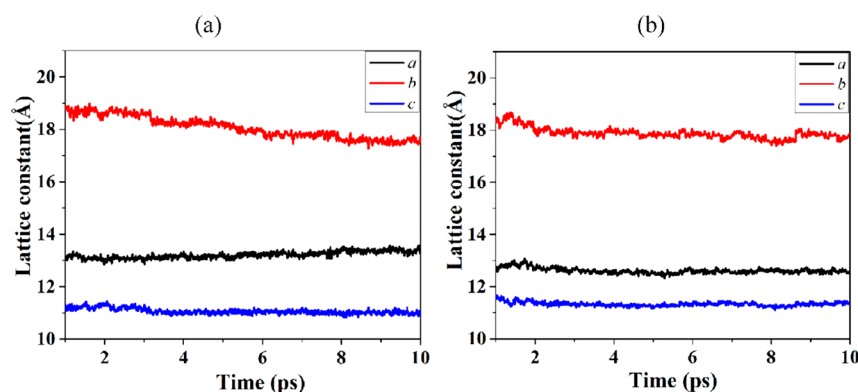


**Figure 2.** Temporal evolution of the lattice constants in the MD simulations performed at (a) 26 GPa and 1000 K and (b) 30 GPa and 500 K.

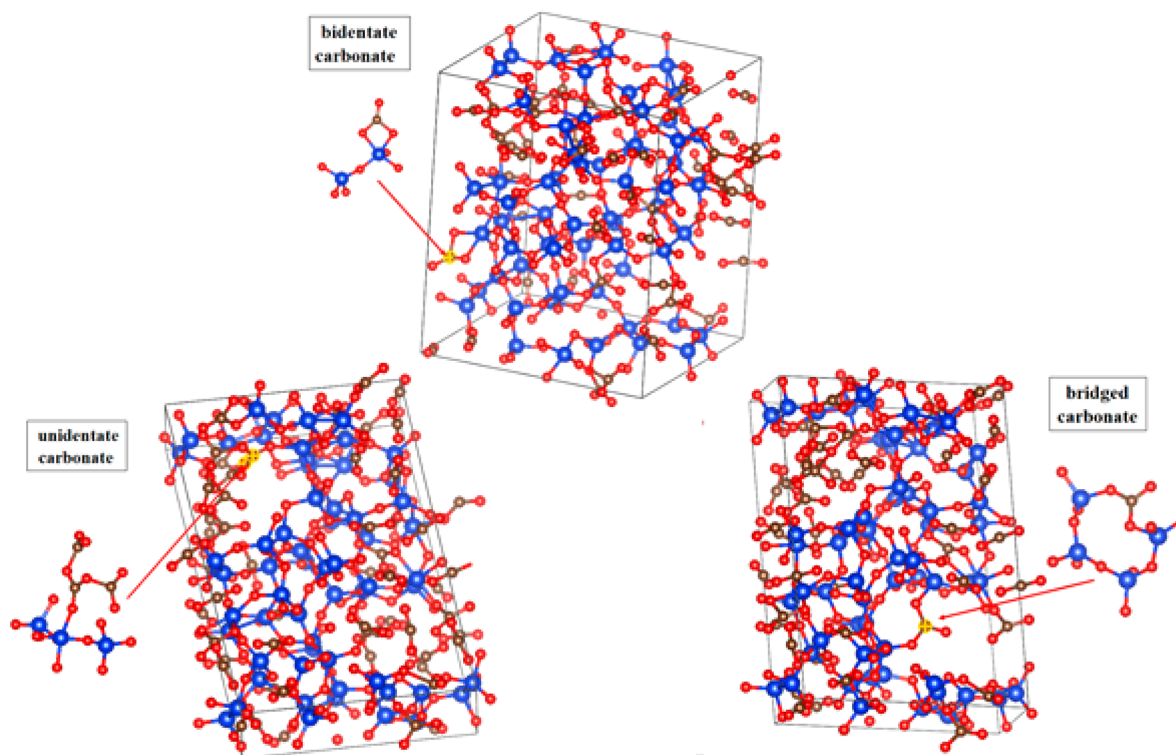


**Figure 3.** Final structure of the  $\text{SiO}_2\text{-CO}_2$  model from the NPT simulation at 1000 K and 26 GPa, with unidentate, bidentate, and bridged carbonate fragments extracted from the final structure.

decreased most noticeably in the  $b$  axes with a small increase in the  $a$  axes (Figure 2a,b). This indicated that the porous  $\text{SiO}_2$  framework had shrunk and the  $\text{SiO}_2$  framework began to distort. At 30 GPa, the  $a$  lattice constant ( $x$ -direction) shortened more than the  $b$  lattice constant, as compared to 26 GPa. In both calculations, the compressed structure helped to bring the  $\text{SiO}_2$  and  $\text{CO}_2$  closer, promoting the initial chemical interaction. Reactions occurred only between  $\text{CO}_2$  and  $\text{SiO}_2$  (Figures 1c,d and 3) on the channel surfaces, forming unidentate, bidentate, and bridged carbonates (Figure 3). This observation is exactly the same as that suggested in the experimental study.<sup>2</sup> After 8 ps, the model system equilibrated and there was no more change in the lattice constants. This is also reflected from the evolution of the total energy with time (Figure S1) where there is little change after 8 ps. No new reactions were detected up to 25 ps. The reason that no more reaction occurs is that the exposed  $\text{SiO}_2$  surface is already covered by reacted  $\text{CO}_2$  and those free molecules are no longer

able to interact with the  $\text{SiO}_2$  and the reaction ceased. Polycarbonate ( $\text{CO}_3$ ) chains composed of  $-\text{O}-(\text{C}=\text{O})-\text{O}-$  were formed in the large channel (10-member  $\text{Si}-\text{O}$  ring channel) with some unreacted  $\text{CO}_2$  molecules. The product consisted of three coordinated carbonate ( $\text{CO}_3$ ) groups with an average  $\text{C}-\text{O}$  bond length of 1.45 Å. Remarkably, even after the reaction, the SFS framework was only slightly distorted, and the gross zeolite structure was maintained (Figure 4). The reactions between  $\text{SiO}_2$  and  $\text{CO}_2$  resulted in an increase in the local  $\text{Si}-\text{O}$  coordination number to five.

To understand the reaction mechanism, we analyzed the temporal atom positions from the MD trajectory. For both simulations (i.e., 26 GPa at 1000 K and 30 GPa at 500 K), similar results were found. The temporal variation of the lattice constants plotted in Figure 2 shows a slowly decreasing trend, indicating that the reaction between  $\text{SiO}_2$  and  $\text{CO}_2$  proceeded gradually. At high pressures and high temperatures, some of the  $\text{CO}_2$  exhibited large-amplitude and fluxional  $\text{O}-\text{C}-\text{O}$  bending

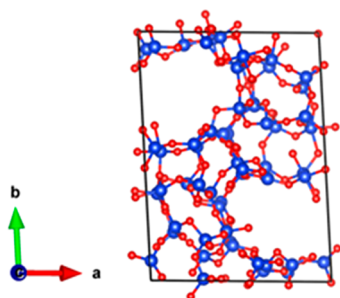


**Figure 4.** SiO<sub>2</sub> framework of the final structure of the SiO<sub>2</sub>–CO<sub>2</sub> model from the *NPT* MD calculation at 26 GPa and 1000 K, with CO<sub>2</sub> molecules and polycarbonate chains removed.

motions, as evidenced by a large O=C=O angle distribution shown in Figure S2. The distribution function has a broad distribution between 150 and 180° showing substantial fluxional bending of the CO<sub>2</sub>. When the bent CO<sub>2</sub> moved closer to the surface of the SiO<sub>2</sub>, forming the channels, the O of CO<sub>2</sub> started to bond with the Si forming 5-Si–O coordinated Si centers (Figure 5a). The C hybridization changed from sp to sp<sup>2</sup>. This initial reaction occurred near the five-membered ring pores. This is not unreasonable as the bent CO<sub>2</sub> needed to migrate only a short distance before reaching the SiO<sub>2</sub> in the channel. The reacted CO<sub>2</sub> was trapped and immobilized in the channels. In the subsequent step, the C reacted with the bridging O of two corner-shared SiO<sub>4</sub> tetrahedra (Si–O–Si linkage) and formed the bidentate carbonates (Figure 5b). The reaction was then paused, and no further reaction was observed for 3.5 ps, even though the lattice constants were decreased further. After 3.5 ps, similar reactions between CO<sub>2</sub> and SiO<sub>2</sub> in the 10-membered ring pores were observed (Figure 5c). Because the large pores (ten-membered ring) are more spacious, the reacted CO<sub>2</sub> can orient parallel to the channel. When more free CO<sub>2</sub> molecules were diffused into the channel, additional reactions were observed (Figure 5d,e). Unidentate carbonates formed when the CO<sub>2</sub> molecules were situated perpendicular to the channel surface (Figure 5d). Bidentate carbonates formed in the large pores (Figure 5d,e). Up to 6.1 ps, the carbonates in the large channels continued to react further when the additional CO<sub>2</sub>, brought closer by diffusion, led to the formation of polycarbonate chains attached to the channel surface (Figure 5f–h). No further reactions (Figure S2) were found even when the MD simulation was extended to 25 ps. A similar reaction mechanism was also observed at 30 GPa and 500 K. Therefore, the pressure and temperature collaborated to drive the chemical reactions.

Examination of the atom trajectories showed that the reaction between CO<sub>2</sub> and SiO<sub>2</sub> can be organized into three stages (Scheme 1). (i) At high temperatures, the CO<sub>2</sub> molecule bends. (ii) The initial reaction was between the O of the CO<sub>2</sub> and the Si of the SiO<sub>4</sub> tetrahedra on the surface of the channels, where the lone pair of the O interacted with the empty σ\* orbital of SiO<sub>2</sub> (see Scheme 2) and the C bonded to the bridging Si–O–Si forming CO<sub>3</sub>. (iii) Finally, subsequent reactions with other free CO<sub>2</sub> produced the polymer structure.

**3.2. Formation of a Cristobalite-like SiO<sub>2</sub>–CO<sub>2</sub> Solid Solution.** Although the high-pressure crystalline polymorphs of CO<sub>2</sub> and SiO<sub>2</sub> share several similar structural features, there is a significant difference in the C–O and Si–O bond lengths. The formation of a SiO<sub>2</sub>–CO<sub>2</sub> crystalline would not intuitively be expected to form a stable cristobalite-like solid, as it would

require both C and Si to have compatible coordination environments. Therefore, it was unexpected that a crystalline solid, composed of similar stoichiometric amounts of CO<sub>2</sub> and SiO<sub>2</sub>, was reported from the reaction of CO<sub>2</sub> with melted zeolite SSZ-56 at 16–22 GPa and 4000 K.<sup>3</sup> Even more remarkably, this new material was shown to be recoverable under close to ambient conditions. X-ray diffraction measurements<sup>3</sup> suggested this new phase can be assigned to an α-cristobalite structure with both C and Si 4-fold coordinated to the O atoms. Later, this conclusion was challenged as it was found that the experimental diffraction pattern may also be attributed to β-ReO<sub>2</sub> due to the reaction of the Re gasket with CO<sub>2</sub> at high pressures and high temperatures.<sup>12</sup> This new finding has led to the retraction of the claim.<sup>3</sup> Nevertheless, it is of great interest to investigate the potential formation of a SiO<sub>2</sub>–CO<sub>2</sub> solid solution.

To explore the possibility of formation of a SiO<sub>2</sub>–CO<sub>2</sub> solid solution, the reaction product of CO<sub>2</sub> in zeolite SSZ-56 described above was melted at 4000 K using an AIMD simulation in the *NVT* ensemble. Quenching of the molten structure was conducted by decreasing the temperature slowly in steps of 100–500 K followed by a long 20 ps annealing. In the melt, both Si and C atoms were found to be distributed evenly (Figure 6). Once quenching had occurred, a structure composed of linked, corner-sharing CO<sub>4</sub> and SiO<sub>4</sub> tetrahedra (the basic structural feature of the cristobalite structure) and the remaining CO<sub>3</sub> were found (Figure 6). It is not surprising or unexpected that the calculations did not reproduce the observed crystal structure. However, the essential structural motif of the SiO<sub>2</sub>–CO<sub>2</sub> solid solution, i.e., the occurrence of linked CO<sub>4</sub> and SiO<sub>4</sub> tetrahedra, was clearly observed. Apparently, it is indeed possible to form a solid with connected CO<sub>4</sub> and SiO<sub>4</sub> tetrahedra.

To examine the stability of the proposed crystalline SiO<sub>2</sub>–CO<sub>2</sub> solid solution, we constructed an α-cristobalite-type structure with equal amounts of CO<sub>2</sub> and SiO<sub>2</sub>, i.e., Si<sub>2</sub>C<sub>2</sub>O<sub>8</sub>. The model was constructed by replacing half of the Si atoms with C atoms randomly. The model structure was then fully optimized at selected pressures. The optimized model has a monoclinic *P2*<sub>1</sub> space group (Figure 7a), but the unit cell angles were very close to 90°. The optimized lattice parameters at 9 GPa were as follows: *a* = 4.389 Å, *b* = 4.181 Å, and *c* = 5.983 Å, β = 90.5°. The theoretical structure, accounting for the distortion in the crystal structure due to the disordered C and Si positions, is in fair agreement with the experimentally observed cristobalite-type tetragonal *P4*<sub>1</sub>2<sub>1</sub>2 structure with *a* (= *b*) = 4.594(1) Å and *c* = 5.938(3) Å at 7 GPa. The result agrees with a previous structural prediction calculation in which a similar *P2*<sub>1</sub> structure is found to be stable at 20 GPa.<sup>10</sup>

Significantly, the predicted structure is dynamically stable (Figure 7b) and can be quenched recoverably, as no soft mode was found in the calculated phonon band structure computed at 0 GPa shown in Figure 7b. The calculated infrared (IR) and Raman spectra at 9 GPa are shown in panels a and b of Figure 8, respectively. Remarkably, the single dominant sharp peak observed<sup>3</sup> at 540 cm<sup>−1</sup> due to C–O–Si bending vibration in the experimental Raman spectrum is reproduced by the calculations. In the calculated Raman spectrum, the peaks around 450 cm<sup>−1</sup> can be assigned to Si–O–Si bending of the zeolite frame; the vibrations in the range of 800–970 cm<sup>−1</sup> belong to the O–C–O bending modes, and the weak peaks at 1060–1150 cm<sup>−1</sup> are the asymmetric ν(C–O–C) stretch modes. In the IR spectrum, the peaks at 600–800 cm<sup>−1</sup> belong

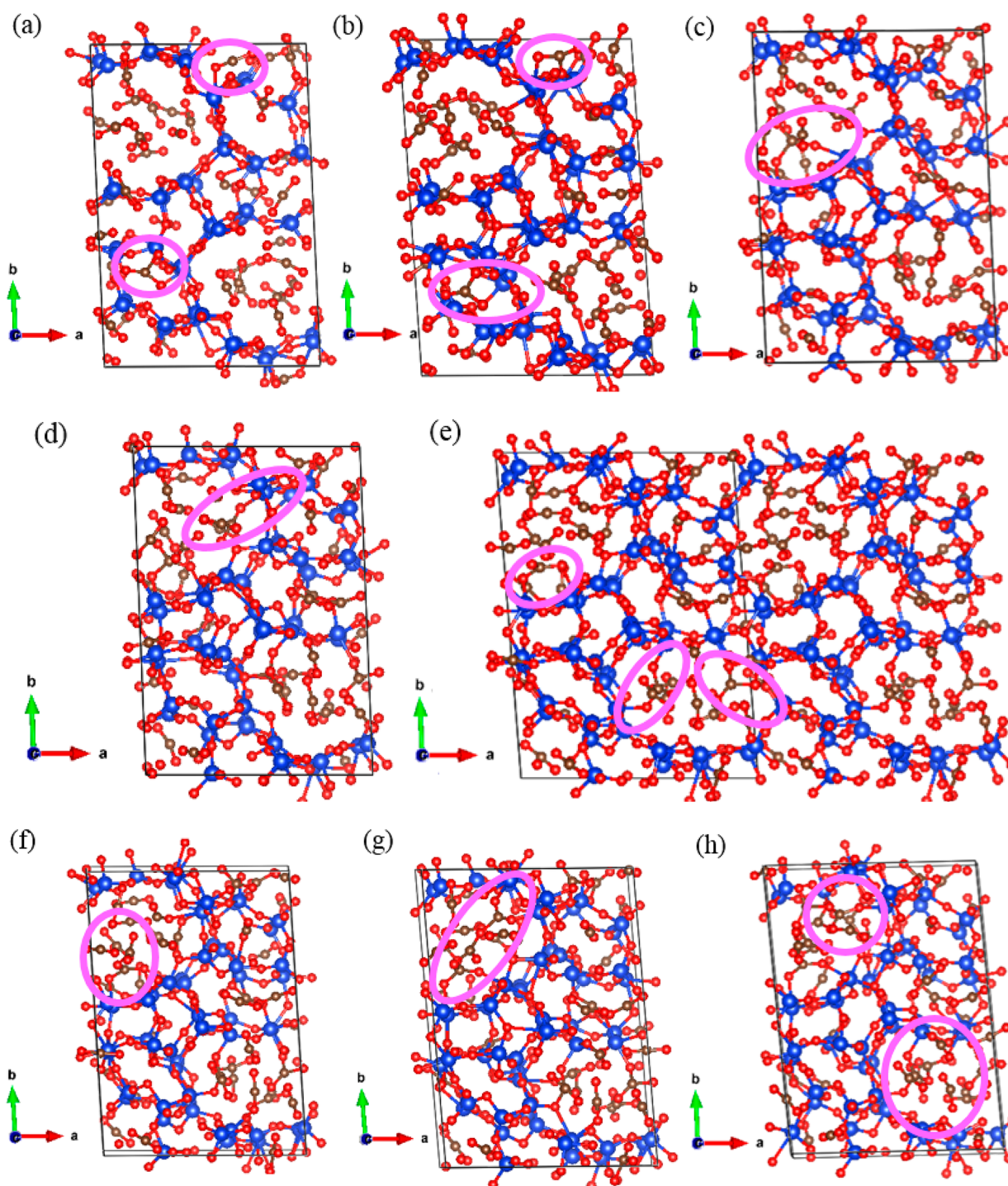
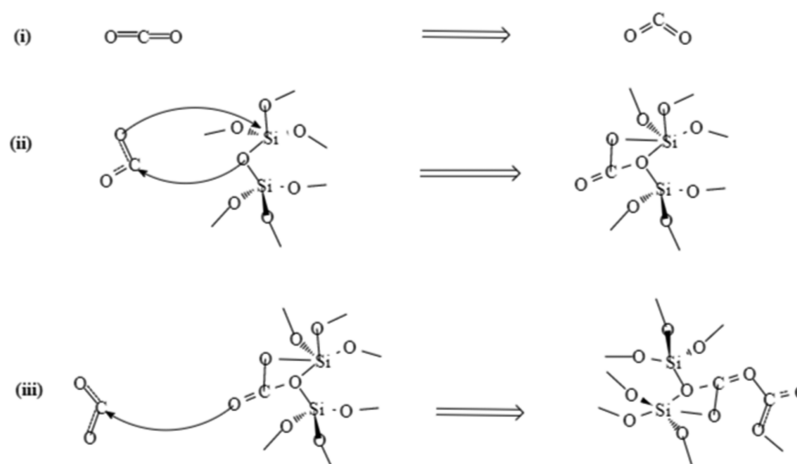


**Figure 5.** Snapshots of the  $\text{SiO}_2\text{-CO}_2$  model system at different stages from the *NPT* calculation at 26 GPa and 1000 K at (a) 479, (b) 749, (c) 3501, (d) 3821, (e) 6101, (f) 6131, (g) 6201, and (h) 8000 fs. The purple circles highlight the structural changes described in the text.

to O–C–O  $\nu_2$  while the peaks at 800–1000 are those of O–Si–O. Peaks at 1100 can be assigned to the Si–O–C mixed stretch modes. The calculated vibration spectra provide the evidence that an  $\alpha$ -cristobalite  $\text{SiO}_2\text{-CO}_2$  solid solution may have been formed in the previous experiment. Noting that the experiment may be contaminated by  $\text{ReO}_2$ ,<sup>11</sup> the theoretical results presented here encourage further experimental work to investigate the possible formation of a  $\text{SiO}_2\text{-CO}_2$  solid solution.

The thermodynamic stability of the  $\text{SiO}_2\text{-CO}_2$  solid solution with the  $\alpha$ -cristobalite structure in the pressure range of 2–25 GPa is determined from a comparison between the calculated enthalpies of the  $\text{SiO}_2\text{-CO}_2$  model and the sum of (i)  $\text{CO}_2\text{-III}$  and quartz and (ii)  $\text{CO}_2\text{-III}$  and  $\alpha$ -cristobalite (Figure 8c). Solid  $\text{CO}_2\text{-III}$  was chosen for reference because it is the stable solid phase in this pressure range. The results show that the solid solution is thermodynamically unstable with respect to  $\text{CO}_2$  and quartz but is thermodynamically stable with respect to  $\text{CO}_2\text{-III}$  and  $\alpha$ -cristobalite. This is reasonable because the

**Scheme 1. Three Primary Reactions of (i) the Bent CO<sub>2</sub> at High Temperatures and High Pressures, (ii) the O of the Bent CO<sub>2</sub> That Bonded with Si of SiO<sub>4</sub> Tetrahedra on the Surface of the Zeolite Channel Forming a Five-Coordinate Si Center, and (iii) the Other O Atom of the CO<sub>2</sub> That Interacted with Additional CO<sub>2</sub> Molecules and Initialized Polymerization**



**Scheme 2. Orbital Interaction Diagram of the Initial Chemical Reaction between CO<sub>2</sub> and SiO<sub>2</sub>**

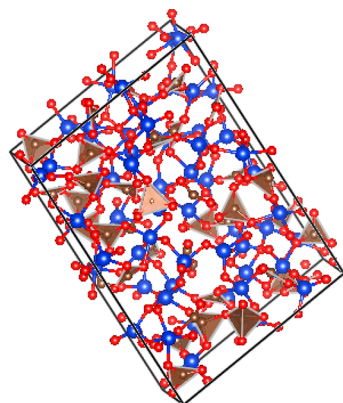
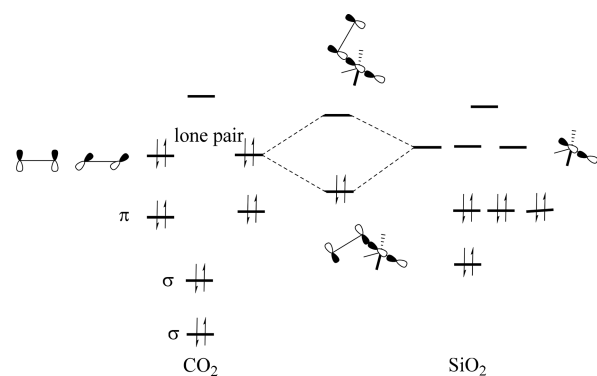


**Figure 6.** SiO<sub>2</sub>-CO<sub>2</sub> model at 26 GPa obtained from melting zeolite SiO<sub>2</sub>-CO<sub>2</sub> at 4000 K and quenched to 500 K. The connected CO<sub>4</sub>-SiO<sub>4</sub> units are shown as shaded tetrahedra.

quartz is the stable phase of the four Si-O coordinated phase.<sup>25</sup> Therefore, in principle, an  $\alpha$ -cristobalite SiO<sub>2</sub>-CO<sub>2</sub> solid solution can form at high temperatures and pressures higher than 10 GPa and become metastable and recoverable under ambient conditions.

The band structure calculation shows this novel SiO<sub>2</sub>-CO<sub>2</sub> solid solution is an insulator with a direct band gap of 6.0 eV (Figure 9a). The band gap is smaller than those of the SiO<sub>2</sub>

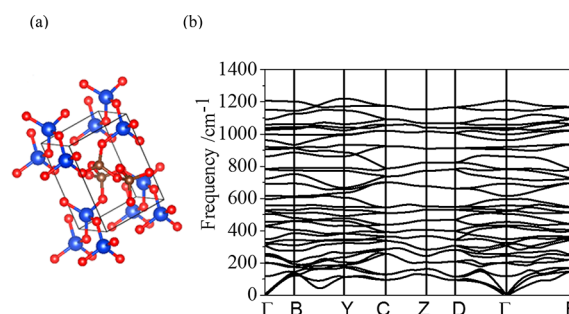


**Figure 7.** (a) Optimized  $\alpha$ -cristobalite-like SiO<sub>2</sub>-CO<sub>2</sub> solid solution at 9 GPa and (b) phonon spectrum for the recovered structure at 0 GPa.

analogues (under ambient conditions, the band gap of polycrystalline SiO<sub>2</sub> is  $8.9 \pm 0.2$  eV;<sup>15</sup> that of the thermally grown amorphous SiO<sub>2</sub> film is 9.3 eV,<sup>26</sup> and that of amorphous SiO<sub>2</sub> is 9.7 eV<sup>26</sup>). Furthermore, crystalline silica  $\alpha$ -quartz,  $\beta$ -quartz,  $\alpha$ -cristobalite,  $\beta$ -cristobalite, and  $\beta$ -tridymite show similar electronic band structures and band gaps.<sup>27-30</sup> In the SiO<sub>2</sub>-CO<sub>2</sub> solid solution, the dispersions of the valence electronic bands are surprisingly flat throughout the entire Brillouin zone. The calculated absorption spectrum (Figure 9b) also shows band-edge absorption around 6.0 eV with a broad main absorption at 12 eV. The reflectivity (Figure 9c) is quite small at a low frequency as the compound is transparent. The calculated low-frequency refractive index is  $n(\omega) = 1.17$ , which is much smaller than that of  $\alpha$ -quartz (1.46).<sup>31</sup> Thus, the SiO<sub>2</sub>-CO<sub>2</sub> solid solution may also be a good glass material. The SiO<sub>2</sub>-CO<sub>2</sub> solid at 0 GPa is predicted to have a bulk modulus  $B$  of 55.62 GPa, which is higher than that of quartz (36.4 GPa).<sup>32</sup> The calculated Vickers hardness ( $H_v$ ) is  $\sim 11.0$  GPa, which is comparable to that of quartz (9.81–11.3 GPa).<sup>33</sup> The larger bulk modulus and hardness compared to those of quartz are due to the stronger C-O bonds in the structure.

#### 4. CONCLUSION

In this study, novel reactions among SSZ-56, a microporous SiO<sub>2</sub> zeolite, and CO<sub>2</sub> molecules trapped in the cavities were observed under the pressure and temperature conditions of the Earth mantle. We have made several contributions. (i) Under high-pressure and -temperature conditions, CO<sub>2</sub> should be a

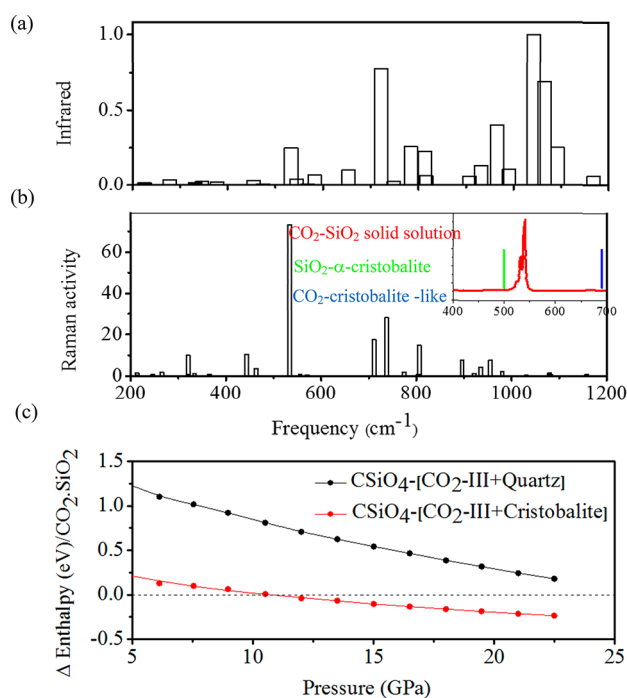


**Figure 8.** Calculated (a) IR and (b) Raman spectra for the studied  $\text{SiO}_2\text{-CO}_2$  solid solution at 0 GPa. The inset is adopted from ref 3, where the red and blue peaks correspond to the  $\text{SiO}_2\text{-}\alpha\text{-cristobalite}$  and cristobalite-like  $\text{CO}_2$ , respectively. (c) Formation enthalpy for the  $\alpha\text{-cristobalite-like}$   $\text{SiO}_2\text{-CO}_2$  solid solution with respect to phase III of  $\text{CO}_2$  and quartz and  $\alpha\text{-cristobalite}$ .

supercritical fluid, yet we found no percolation of  $\text{CO}_2$  into the bulk solid. Chemical reactions were observed at 26 GPa and

1000 K with only the  $\text{SiO}_2$  on the surface of the cavities of zeolite SSZ-56. (ii) The vibrational modes of the chemical species proposed in the experimental Raman and infrared spectra are identified. (iii) The mechanisms of formation of these species, particularly the polycarbonates, are elucidated from the analysis of the molecular dynamics trajectories. It was found that the formation of 5 Si–O coordinated Si atoms plays a critical role in promoting the reactions between  $\text{CO}_2$  and  $\text{SiO}_2$ . The reactions occurred only at the pore surface through an initial interaction between the Si and O with a thermally excited bent  $\text{CO}_2$ . Subsequent reactions eventually led to the formation of polycarbonate chains. (iv) We provided energetic and spectroscopic evidence of the formation of the  $\text{CO}_2\text{-SiO}_2$  solid solution upon cooling from the melt. The thermodynamic stability of the cristobalite structure above 9 GPa is confirmed with the calculated Raman spectrum in substantial agreement with experiment. The theoretical results lend support to the possible synthesis and existence of this novel structure that has been suggested earlier. The solid solution is also predicted to be quench recoverable. It is a hard material with interesting electronic properties. The new results will potentially stimulate further experimental exploration of this system.

## ■ ASSOCIATED CONTENT

### Supporting Information

The Supporting Information is available free of charge on the ACS Publications website at DOI: [10.1021/acsearthspacechem.7b00144](https://doi.org/10.1021/acsearthspacechem.7b00144).

Evolution of temperature and total energy of  $\text{SiO}_2\text{-CO}_2$  from NPT simulation at 26 GPa and 1000 K (Figure S1) and O–C–O angle distribution of the product from the chemical reactions at 26 GPa and 1000 K (Figure S2) (PDF)

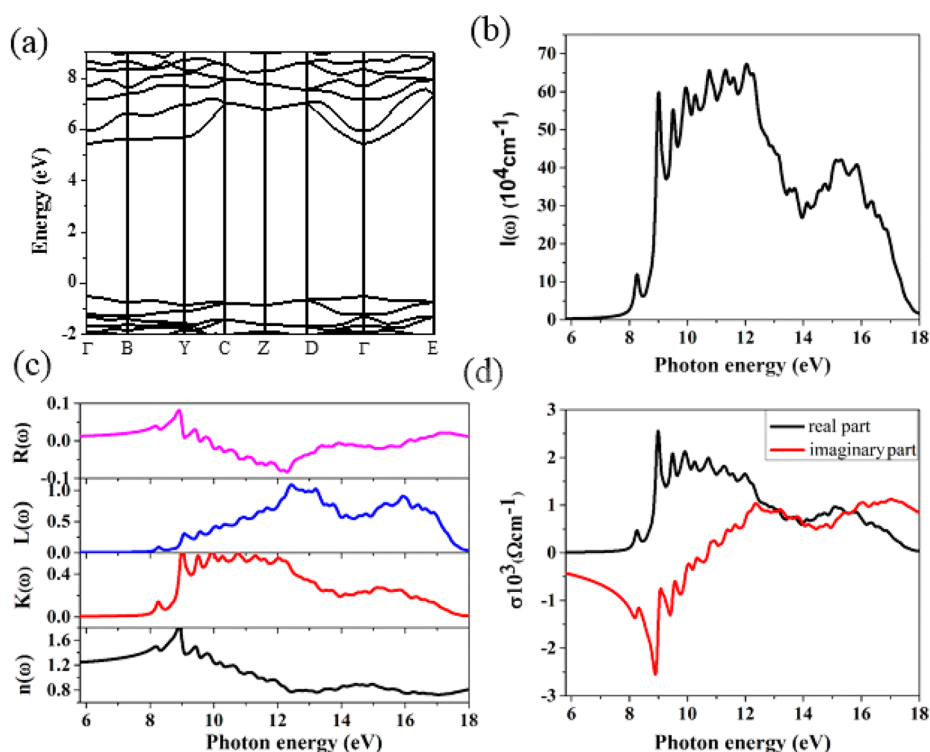


**Figure 9.** Calculated (a) electronic band structure, (b) absorption spectrum, (c) refractive index, energy-loss spectrum, extinction coefficient, and refractive index, and (d) optical conductivity for the cristobalite-like  $\text{SiO}_2\text{-CO}_2$  solid structure.

Crystallographic data (CIF)

## AUTHOR INFORMATION

### Corresponding Author

\*E-mail: john.tse@usask.ca.

### ORCID

Xue Yong: 0000-0002-2134-7519

### Notes

The authors declare no competing financial interest.

## ACKNOWLEDGMENTS

The authors acknowledge WestGrid for providing computational resources.

## REFERENCES

- (1) Yoo, C.-S. Physical and chemical transformations of highly compressed carbon dioxide at bond energies. *Phys. Chem. Chem. Phys.* **2013**, *15* (21), 7949–7966.
- (2) Santoro, M.; Gorelli, F.; Haines, J.; Cambon, O.; Levelut, C.; Garbarino, G. Silicon carbonate phase formed from carbon dioxide and silica under pressure. *Proc. Natl. Acad. Sci. U. S. A.* **2011**, *108* (19), 7689–7692.
- (3) Santoro, M.; Gorelli, F. A.; Bini, R.; Salamat, A.; Garbarino, G.; Levelut, C.; Cambon, O.; Haines, J. Carbon enters silica forming a cristobalite-type CO<sub>2</sub>-SiO<sub>2</sub> solid solution. *Nat. Commun.* **2014**, *5*, 3761–3765.
- (4) Matter, J. M.; Stute, M.; Snæbjörnsdóttir, S. Ó.; Oelkers, E. H.; Gislason, S. R.; Aradóttir, E. S.; Sigfusson, B.; Gunnarsson, I.; Sigurdardóttir, H.; Gunnlaugsson, E.; et al. Rapid carbon mineralization for permanent disposal of anthropogenic carbon dioxide emissions. *Science (Washington, DC, U. S.)* **2016**, *352* (6291), 1312–1314.
- (5) House, K. Z.; Schrag, D. P.; Harvey, C. F.; Lackner, K. S. Permanent carbon dioxide storage in deep-sea sediments. *Proc. Natl. Acad. Sci. U. S. A.* **2006**, *103* (33), 12291–12295.
- (6) Washbourne, C. L.; Renforth, P.; Manning, D. A. C. Investigating carbonate formation in urban soils as a method for capture and storage of atmospheric carbon. *Sci. Total Environ.* **2012**, *431*, 166–175.
- (7) Ghosh, D. B.; Bajgain, S. K.; Mookherjee, M.; Karki, B. B. Carbon-bearing silicate melt at deep mantle conditions. *Sci. Rep.* **2017**, *7* (1), 848–854.
- (8) Morales-García, A.; Marqués, M.; Menéndez, J. M.; Santamaría-Pérez, D.; Baonza, V. G.; Recio, J. M. First-principles study of structure and stability in Si–C–O-based materials. *Theor. Chem. Acc.* **2013**, *132* (1), 1308.
- (9) Qu, B.; Li, D.; Wang, L.; Wu, J.; Zhou, R.; Zhang, B.; Zeng, X. C. Mechanistic study of pressure and temperature dependent structural changes in reactive formation of silicon carbonate. *RSC Adv.* **2016**, *6* (32), 26650–26657.
- (10) Zhou, R.; Qu, B.; Dai, J.; Zeng, X. C. Unraveling Crystalline Structure of High-Pressure Phase of Silicon Carbonate. *Phys. Rev. X* **2014**, *4* (1), 11030.
- (11) Santoro, M.; Gorelli, F. A.; Bini, R.; Salamat, A.; Garbarino, G.; Levelut, C.; Cambon, O.; Haines, J. Correspondence: Reply to “Strongly-driven Re+CO<sub>2</sub> redox reaction at high-pressure and high-temperature. *Nat. Commun.* **2016**, *7*, 13538.
- (12) Santamaria-Perez, D.; McGuire, C.; Makhlof, A.; Kavner, A.; Chulíá-Jordan, R.; Jorda, J. L.; Rey, F.; Pellicer-Porres, J.; Martinez-García, D.; Rodríguez-Hernández, P.; et al. Correspondence: Strongly-driven Re+CO<sub>2</sub> redox reaction at high-pressure and high-temperature. *Nat. Commun.* **2016**, *7*, 13647.
- (13) Elomari, S.; Burton, A.; Medrud, R. C.; Grosse-Kunstleve, R. The synthesis, characterization, and structure solution of SSZ-56: An extreme example of isomer specificity in the structure direction of zeolites. *Microporous Mesoporous Mater.* **2009**, *118* (1–3), 325–333.
- (14) Hill, R. The Elastic Behaviour of a Crystalline Aggregate. *Proc. Phys. Soc., London, Sect. A* **1952**, *65* (5), 349.
- (15) DiStefano, T. H.; Eastman, D. E. The band edge of amorphous SiO<sub>2</sub> by photoinjection and photoconductivity measurements. *Solid State Commun.* **1971**, *9* (24), 2259–2261.
- (16) Kresse, G.; Furthmüller, J. Efficiency of ab-initio total energy calculations for metals and semiconductors using a plane-wave basis set. *Comput. Mater. Sci.* **1996**, *6* (1), 15–50.
- (17) Kresse, G.; Hafner, J. Ab initio molecular dynamics for liquid metals. *Phys. Rev. B: Condens. Matter Mater. Phys.* **1993**, *47* (1), 558–561.
- (18) Kresse, G.; Hafner, J. Ab initio molecular-dynamics simulation of the liquid-metal–amorphous-semiconductor transition in germanium. *Phys. Rev. B: Condens. Matter Mater. Phys.* **1994**, *49* (20), 14251–14269.
- (19) Kresse, G.; Furthmüller, J. Efficient iterative schemes for ab initio total-energy calculations using a plane-wave basis set. *Phys. Rev. B: Condens. Matter Mater. Phys.* **1996**, *54* (16), 11169.
- (20) Kresse, G.; Joubert, D. From ultrasoft pseudopotentials to the projector augmented-wave method. *Phys. Rev. B: Condens. Matter Mater. Phys.* **1999**, *59* (3), 1758–1775.
- (21) Perdew, J. P.; Burke, K.; Ernzerhof, M. Generalized Gradient Approximation Made Simple. *Phys. Rev. Lett.* **1996**, *77* (18), 3865–3868.
- (22) Haines, J.; Cambon, O.; Levelut, C.; Santoro, M.; Gorelli, F.; Garbarino, G. Deactivation of Pressure-Induced Amorphization in Silicalite SiO<sub>2</sub> by Insertion of Guest Species. *J. Am. Chem. Soc.* **2010**, *132* (26), 8860–8861.
- (23) Holewinski, A.; Sakwa-Novak, M. A.; Jones, C. W. Linking CO<sub>2</sub> Sorption Performance to Polymer Morphology in Aminopolymer/Silica Composites through Neutron Scattering. *J. Am. Chem. Soc.* **2015**, *137* (36), 11749–11759.
- (24) Yong, X.; Tse, J.; Chen, J. Chemical reaction between CO<sub>2</sub> with quartz and stishovite, manuscript in preparation.
- (25) Zhang, J.; Li, B.; Utsumi, W.; Liebermann, R. In situ X-ray observations of the coesite-stishovite transition: reversed phase boundary and kinetics. *Phys. Chem. Miner.* **1996**, *23* (1), 1–10.
- (26) Nithianandam, V. J.; Schnatterly, S. E. Soft-x-ray emission and inelastic electron-scattering study of the electronic excitations in amorphous and crystalline silicon dioxide. *Phys. Rev. B: Condens. Matter Mater. Phys.* **1988**, *38* (8), 5547–5553.
- (27) Li, Y. P.; Ching, W. Y. Band structures of all polycrystalline forms of silicon dioxide. *Phys. Rev. B: Condens. Matter Mater. Phys.* **1985**, *31* (4), 2172–2179.
- (28) Xu, Y.; Ching, W. Y. Electronic and optical properties of all polymorphic forms of silicon dioxide. *Phys. Rev. B: Condens. Matter Mater. Phys.* **1991**, *44* (20), 11048–11059.
- (29) Ramos, L. E.; Furthmüller, J.; Bechstedt, F. Quasiparticle band structures and optical spectra of beta-cristobalite SiO<sub>2</sub>. *Phys. Rev. B: Condens. Matter Mater. Phys.* **2004**, *69* (8), 85102.
- (30) Sevik, C.; Bulutay, C. Theoretical study of the insulating oxides and nitrides: SiO<sub>2</sub>, GeO<sub>2</sub>, Al<sub>2</sub>O<sub>3</sub>, Si<sub>3</sub>N<sub>4</sub>, and Ge<sub>3</sub>N<sub>4</sub>. *J. Mater. Sci.* **2007**, *42* (16), 6555–6565.
- (31) Malitson, I. H. Interspecimen Comparison of the Refractive Index of Fused Silica\*. *J. Opt. Soc. Am.* **1965**, *55* (10), 1205.
- (32) Quartz Crystal (SiO<sub>2</sub>). <http://www.crystran.co.uk/optical-materials/quartz-crystal-sio2>.
- (33) Osburn, H. J. WEAR OF ROCK-CUTTING TOOLS. *Powder Metall.* **1969**, *12* (24), 471–502.